Hemanth et al. 2016. *Int. J. Vehicle Structures & Systems*, 8(2), 67-73
ISSN: 0975-3060 (Print), 0975-3540 (Online)
doi: 10.4273/ijvss.8.2.02

International Journal of Vehicle Structures & Systems
Available online at www.maftree.org/eja

Inter-laminar Strength of Bonded Composite Lap Joints with Selective Stitching Through the Thickness

R.H. Hemanth and G.V.V. Ravi Kumar[a]

Infosys Limited, Electronic City, Hosur Road, Bangalore, India
[a]Corresponding Author, Email: ravikumar_gvv@infosys.com

ABSTRACT:

In bonded composite lap joints, inter-laminar strength is critical to prevent the delamination. In this paper, the phenomenon of progressive delamination in lap joints is simulated in ABAQUS software using stress based composite failure model. It is observed that in all the joints, failure initiation is due to high inter-laminar stresses at the edges of the lap joint. Use of through the thickness stitching results in a significant improvement in inter-laminar strength in joints. These joints are further analyzed for "selective stitching" wherein the stitching is restricted to the failure regions. The results show that selective stitching is able to provide failure strengths close to that of fully stitched model.

KEYWORDS:

Inter-laminar strength; Composite stitching; Composite lap joints; ABAQUS; USDFLD

CITATION:

R.H. Hemanth and G.V.V. Ravi Kumar. 2016. Inter-laminar Strength of Bonded Composite Lap Joints with Selective Stitching Through the Thickness, *Int. J. Vehicle Structures & Systems*, 8(2), 67-73. doi:10.4273/ijvss.8.2.02

NOMENCLATURE:

E_{11}	Ply Young's modulus in fiber direction
E_{22}	Ply Young's modulus in matrix direction
E_{33}	Ply Young's modulus in inter-laminar direction
G_{12}	Ply shear modulus for fiber to matrix
G_{13}	Ply shear modulus for fiber to inter-laminar
G_{23}	Ply shear modulus for matrix to inter-laminar
ν_{12}	Ply Poisson's ratio for fiber to matrix
ν_{13}	Ply Poisson's ratio for fiber to inter-laminar
ν_{23}	Ply Poisson's ratio for matrix to inter-laminar
S_{XT}	Allowable fiber stress in tension
S_{XC}	Allowable fiber stress in compression
S_{YT}	Allowable matrix stress in tension
S_{YC}	Allowable matrix stress in compression
S_{ZT}	Allowable inter-laminar stress in tension
S_{ZC}	Allowable inter-laminar stress in compression
S_{XZ}, S_{YZ}	Allowable inter-laminar shear stresses
S_{11}	Stress in fiber direction
S_{22}	Stress in matrix direction
S_{33}	Stress in inter-laminar direction
S_{12}	In plane ply shear stress
S_{13}, S_{23}	Inter-laminar shear stresses

1. Introduction

Composite stitching is a process wherein individual composite plies are stitched together in thickness direction using high strength fibers. Stitching is an effective method for joining stacked plies along their edges for easier handling of preform. Stitching also increases the fiber volume fraction in thickness direction, thus improving inter-laminar strength and damage tolerance. The stitching is carried out generally using sewing machines either manually controlled or through an automated process. Stitches behave similar to other 3D composites reinforcements like weaving, braiding and knitting. General types of stitches used are lock, modified lock and chain, which are used based on specific requirements. Stitched composites are now widely used in aircraft industry components like fuselage, wing skin panels and also in automotive industry for floor panels, doors etc.

Stitching in composites was first studied during early 1980s to provide through thickness reinforcement to composite joints [1]. Initial studies revealed that the strength of stitched joints was improved. Many studies are available in the literature both at micro level (interaction between stitch fiber and the surrounding composite) and macro level (overall failure load prediction). Main focus of these studies were on damage tolerance and inter-laminar strength improvement. Prior studies were done at a macro level where samples were physically tested to observe these effects. Many papers infer that due to stitching, the laminate tensile strength improvement is either negligible or marginally degraded [1-3]. This can be attributed to damage of in-plane fibers due to stitching causing misalignment from the load direction. There are some instances where compressive and flexural strengths have shown improvement by stitching [4].

However there is an improvement in inter-laminar behaviour in the range from 15% to 20% [1, 5, and 6] due to the stitches by inhibiting the delamination growth process. The same has been confirmed by other researchers [1] after correlating finite element model with experimental data. The improvement in inter-laminar strength is also seen in stitched sandwich panels [7, 8]. Studies have also been done on the improvements in damage tolerance by stitching. Pang et. al. [9], with two dimensional mechanics model showed that stitched composite has better creep performance by increasing the load and time required to produce same level of

strains as that of unstitched ones. Improvements in fatigue life due to stitching were also observed [1, 10-12]. During the crack propagation, formation of 'stitch bridging zone' by the stitches support a large amount of the stress and reduces energy rate, resulting in reduced crack growth rate [1,4,13-15] and improving impact resistance and post impact properties [1,3,16].

Most of the studies on damage tolerance and impact resistance were based on combination of physical testing and finite element methods. Regarding the delamination and strength prediction, the available literature is based on failure due to crack initiation and propagation. As an alternative approach, the current paper focuses on adopting stress based composite failure theories to simulate the progressive delamination failure. The adopted approach is suitable for quick studies with reasonable accuracy.

2. Methodology

A typical composite lap joint consisting of fiber layers of different angles stacked and bonded with matrix is analyzed to study the effect of stitching. The joint is subjected to displacement loading with material and geometric nonlinearity. Sensitivity analysis of the joint is done with following parameters:

1) Unstitched, stitched and selectively stitched
2) Stitch pitches (2, 4, 6, 8 and 12 mm)
3) Single and double lap joints
4) Stitch fibers (Kevlar and Carbon)

ABAQUS software is used for failure simulation which has good nonlinear (material and geometric) analysis capabilities and has subroutines capable of simulating user defined composites failures models [17].

2.1. Test model

The lap joint model consists of laminates made of Carbon Fiber Reinforced Plastic (CFRP) piles of 0.4mm thickness. The dimensions of the lap joints are shown in Fig. 1 and the ply details are summarized in Table 1.

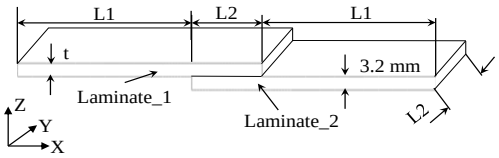

a) Single lap joint (L1 = 60 mm, L2 = 24.4 mm, t = 3.2 mm)

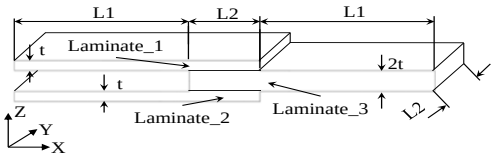

b) Double lap joint (L1 = 60 mm, L2 = 24.4 mm, t = 3.2 mm)

Fig. 1: Details of lap joint models

Table 1: Laminate details of lap joints

Laminate name	No. of layers	Stacking Sequence
Laminate_1 & Laminate_2	8	$[0/+45/-45/0]_S$
Laminate_3	16	$[0/+45/-45/90/90/-45/+45/0]_S$

In all the lap joints, the stitching is limited to the overlapping area. A typical stitched lap joint model is shown Fig. 2. However joint is extended by 0.2 mm to cover the extreme stitches.

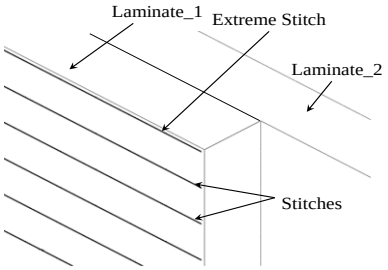

Fig. 2: Typical through the thickness stitching details in a single lap joint

2.2. Material properties

T300/Epoxy is considered as ply material. The ply properties are obtained from literature [18] and are given in Table 2. The 0° fiber is aligned along X axis and stacking direction is in Z axis. The stitching is done using Kevlar fibers of 1000 Denier and the properties considered [19] are shown in Table 3.

Table 2: T300/Epoxy material details

Properties	Values
Mass density	1.6E-09 Tonnes/mm³
E_{11}	181GPa
E_{22}, E_{33}	10.3 GPa, 10.3 GPa
ν_{12}, ν_{13}, ν_{23}	0.28
G_{12}, G_{13}, G_{23}	7.17GPa, 7.17GPa, 1.31GPa
S_{XT} & S_{XC}	1500 MPa (tensile and compressive)
S_{YT}, S_{YC}, S_{XZ} & S_{YZ}	40 MPa (tensile), 246 MPa (compressive) and 68 MPa (shear)

Table 3: Stitch fiber material details

Properties	Values
Mass density	1.44E-09 Tonnes/mm³
E_{11}	124 GPa
ν_{12}	0.32
S_{XT}	3600 MPa

2.3. Failure implementation

Material failure is simulated in the analysis to observe the composite failure initiation and progression for various cases. The USDFLD subroutine [17] is used in ABAQUS to implement stress based failure at the element integration point level. Various modes of composite failure are considered in the analysis, as shown in Table 4 to Table 6. At the end of each converged iteration, the USDFLD subroutine extracts the stress components at element integration points and compares them with the corresponding user defined allowable. If any of the criteria is satisfied, the subroutine will degrade the material properties of the corresponding element integration point based on the type of failure. The element stiffness matrix is updated for the next iteration using the degraded material properties. The process is repeated until the model is not able to carry further load due to complete failure. At this juncture, the run will experience non-convergence and will abort. For stitch material, linear stress behaviour is considered with instantaneous failure as soon as the stress reaches the allowable tensile strength.

Table 4: In-plane failure criteria

Failure criterion	Equation	Material properties nullified
Stress based fiber failure	$\left(\frac{S_{11}}{S_{xT}}\right) \geq 1$, if S_{11} is tensile $\left(\frac{S_{11}}{-S_{xC}}\right) \geq 1$, if S_{11} is compressive	All properties
Stress based matrix failure	$\left(\frac{S_{22}}{S_{YT}}\right) \geq 1$, if S_{22} is tensile $\left(\frac{S_{22}}{-S_{YC}}\right) \geq 1$, if S_{22} is compressive	All except E_{11}

Table 5: Inter-laminar failure criteria

Failure criterion	Equation	Material properties nullified
Stress based failure	$\left(\frac{S_{13}}{S_{xz}}\right)^2 + \left(\frac{S_{23}}{S_{yz}}\right)^2 + \left(\frac{S_{33}}{S_{zT}}\right)^2 \geq 1$, if S_{33} is tensile $\left(\frac{S_{13}}{S_{xz}}\right)^2 + \left(\frac{S_{23}}{S_{yz}}\right)^2 + \left(\frac{S_{33}}{S_{zC}}\right)^2 \geq 1$, if S_{33} is compressive	E_{33}, ν_{13}, ν_{23}, G_{13}, G_{23}

Table 6: Combined failure criteria

Failure criterion	Material properties nullified
Combined fiber and matrix	All properties
Combined fiber and inter-laminar	All properties
Combined matrix and inter-laminar	All except E_{11}
All failures	All properties

2.4. FE models

The typical mesh of the unstitched model is shown in Fig. 3. The model is meshed with ABAQUS three dimensional 8 noded solid elements (C3D8). The critical regions are fine meshed and are tied to the coarsely meshed non-critical regions as shown in Fig. 3. All the solid elements are aligned to the stacking direction (Z axis). For stitches, rod elements (T3D2) are inserted at regular intervals in between solid elements as shown in Fig. 4. These elements share the nodes with the surrounding solid elements. The mesh details are summarized in Table 7.

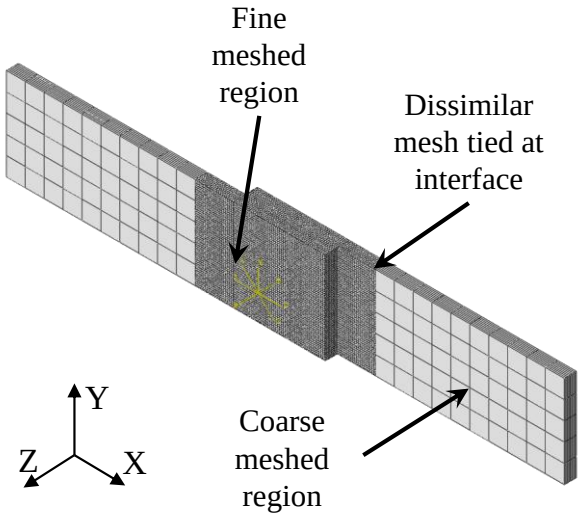

Fig. 3: Lap joint mesh

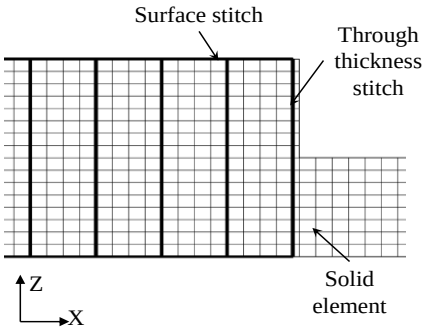

Fig. 4: Representation of stitch fibers in FE model

Table 7: FE mesh summary

a) Ply elements (all models)

Element type	No. of elements / nodes	DOFs	Average element length, mm
C3D8	56800 / 63765	Ux, Uy, Uz	0.387

a) Stitch elements

Model	Element type	No. of elements	DOFs
Stitched with 2 mm pitch	T3D2	3952	Ux, Uy, Uz
Stitched with 4 mm pitch		1456	
Stitched with 6 mm pitch		880	
Stitched with 8 mm pitch		640	
Stitched with 12 mm pitch		452	

2.5. Loading and boundary conditions

Test specimens have been simulated with appropriate loading and boundary conditions [1]. For single lap joints, the Laminate_1 is constrained full face at one end and displacement loading is applied full face on the other end of Laminate_2 as shown in Fig. 5. For double lap joints, additional symmetry conditions are applied on the lower surface of Laminate_2 as shown in Fig. 5. In addition the stitches of lower surface of Laminate_2 (refer Fig. 4) are removed. The end faces are constrained from moving in other directions. The load increment is maintained at not more than 0.01 mm. Once the failure initiation is detected, USDFLD subroutine will cut back the current increment further by factor of 0.01 and rerun with smaller increments. This is helpful in accurately capturing the failure initiation load.

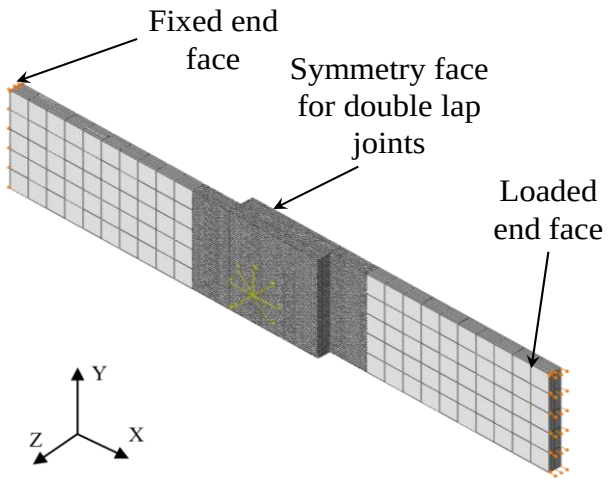

Fig. 5: Loading and boundary conditions

3. Results and discussion

3.1. Effect of stitching

Results of single lap joint unstitched and stitched with 2mm pitch models were analyzed to assess the effect of stitching. Ply wise stresses were extracted at different sections in the lap joint as shown in Fig. 6 and stresses of interface plies in Table 8. Stress components S_{11}, S_{33} and S_{13} were extracted at failure initiation load corresponding to the unstitched model. Ply wise stress results show that the stitching is found to have negligible influence on S_{11} & S_{13}. Its major contribution is reducing the S_{33} stress component in stitched lap joint thus delaying the failure.

The reaction force vs. applied displacement plotted in Fig. 7 shows that the overall in-plane stiffness in the unstitched and stitched models are same till the failure initiation. Thus the stitching is not contributing to the overall in-plane stiffness. Strains were checked at the center of the lap joint and the strain patterns were similar between the models till the ultimate failure of unstitched model. Thus the load path is not affected by stitching.

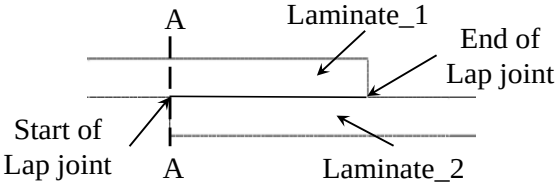

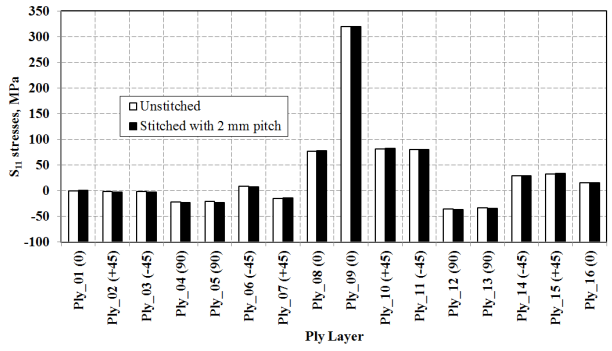

Fig. 6(a):Ply wise S_{11} stresses

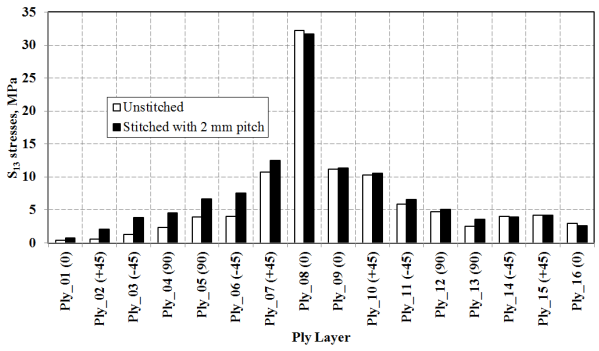

Fig. 6(b):Ply wise S_{13} stresses

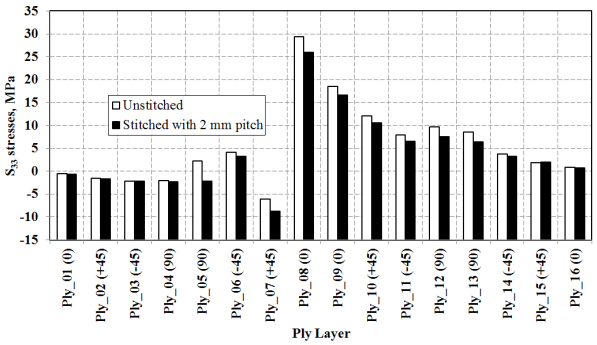

Fig. 6(c): Ply wise S_{33} stresses

Table 8: Stresses at the innermost plies

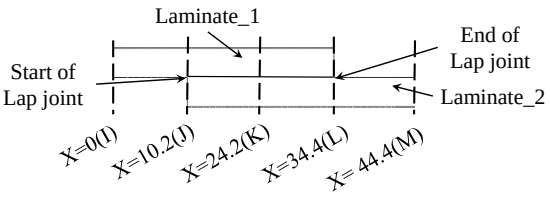

Table 8(a): S_{11} stresses (MPa) at the inner most plies

X location	Upper ply of interface		Lower ply of interface	
	Unstitched	Stitched	Unstitched	Stitched
I	302.8	309.3	-	-
J	382.4	390.7	76.7	76.8
K	122.4	124.1	123.8	125.5
L	76.7	76.8	310.3	317.0
M	-	-	302.8	309.3

Table 8(b): S_{13} stresses (MPa) at the inner most plies

X location	Upper ply of interface		Lower ply of interface	
	Unstitched	Stitched	Unstitched	Stitched
I	0.2	0.2	-	-
J	23.2	23.1	32.0	31.8
K	2.1	2.3	1.6	1.5
L	32.0	31.8	11.1	11.5
M	-	-	0.2	0.2

Table 8(c): S_{33} stresses (MPa) at the inner most plies

X location	Upper ply of interface		Lower ply of interface	
	Unstitched	Stitched	Unstitched	Stitched
I	0.3	0.3	-	-
J	14.6	13.7	28.7	22.7
K	-0.7	0.1	-0.7	0.1
L	28.7	22.7	18.2	16.1
M	-	-	0.3	0.3

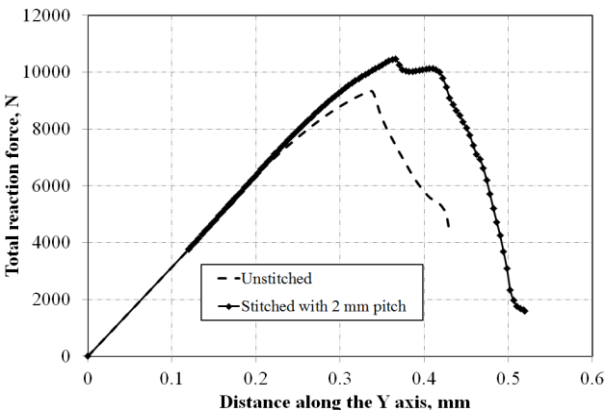

Fig. 7: Reaction force vs. Applied displacement load

In unstitched models, the failure starts in inter-laminar direction in the elements of innermost plies at the edges of the overlap due to high S_{33} and S_{13} stresses occurring at the lap end, as shown in Fig. 8(a). With increasing load, the failure zone then progresses towards the rest of the interface as shown in Fig. 8(b). However in the stitched model, the initiation of inter-laminar failure is delayed compared to unstitched model. Stresses at the edge of the lap were compared at the failure initiation load corresponding to the unstitched model as shown in Fig. 9. The stress comparison shows significant and marginal drops in S_{33} and S_{13} respectively in locations where the stitches are present. Hence for the load at which inter-laminar failure starts in unstitched model, stitched models will not show failure.

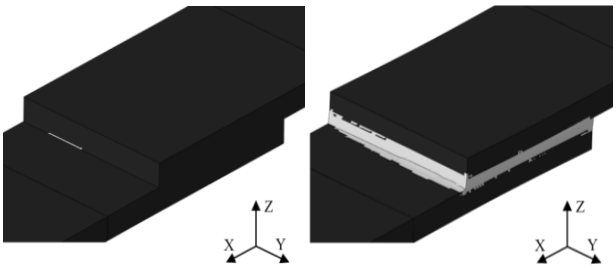

a) Failure initiation **b) Failure At the end of analysis**

Fig. 8: Failure in single lap unstitched model

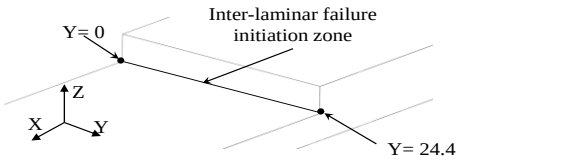

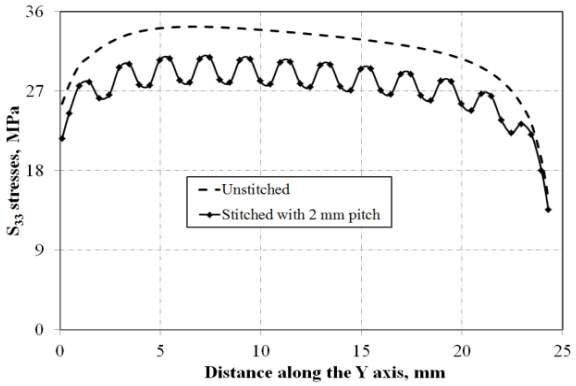

a) S_{33} stresses

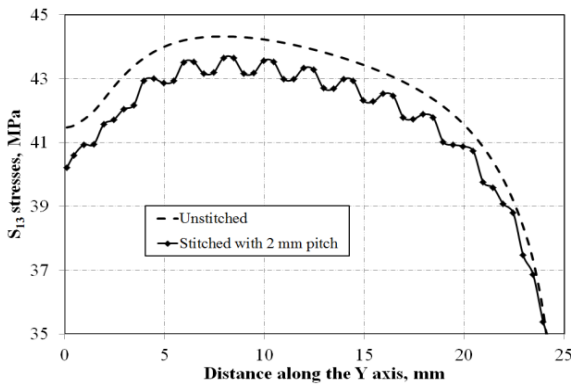

b) S_{13} stresses

Fig. 9: Inter-laminar stresses S_{33} & S_{13} at the failure initiation zone

With increasing load in stitched model, the elements between the stitches fail as shown in Fig. 10(a). The failure gradually spreads to the elements attached to the stitches and proceeds towards the center of the lap and rest of the layers as shown in Fig. 10(b). The progress of delamination is estimated with respect to the applied displacement load for single lap joint models and is shown in Fig. 11. The stitched model shows the delayed failure onset compared to unstitched models. Thus to attain a specified delamination length, the required load is higher for the stitched model.

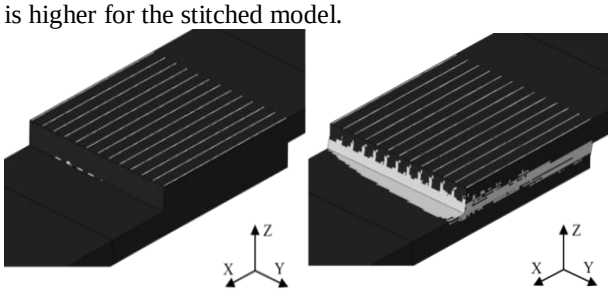

a) Failure initiation **b) Failure At the end of analysis**

Fig. 10: Failure in single lap model with 2mm pitch stitching

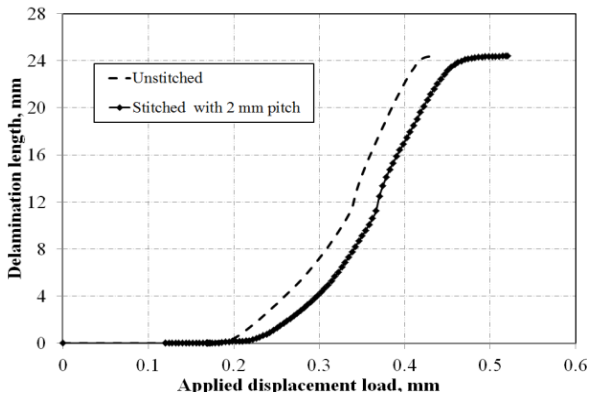

a) Delamination length vs. Applied displacement load

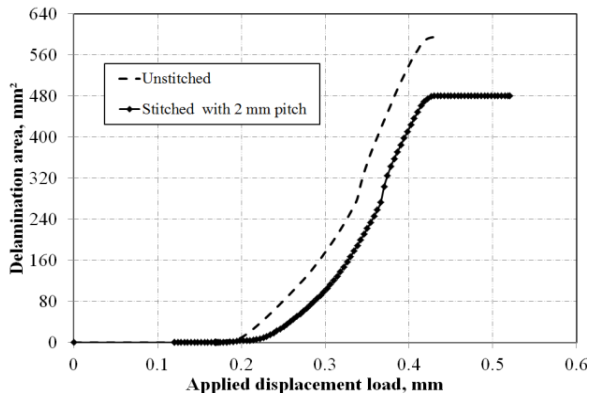

b) Delamination area vs. Applied displacement load

Fig. 11: Progression of failure in single lap models

Axial stresses were studied in the stitches and in all the models ultimate failure happens before the yielding of the stitches. The stitches at the edge of the lap experience high tensile stresses due to onset of inter-laminar failure. The compressive stresses are significant only when the inter-laminar failure is crosses the half lap length. The failure strengths (total reaction forces) are compared with respect to unstitched model in Fig. 12. The range of improvement in failure strengths are summarized in Table 9.

Table 9: Failure strength improvements due to stitching effect

Lap joints	Maximum improvement %	Maximum improvement Model	Minimum improvement %	Minimum improvement Model
Failure initiation strength				
Single	8.7	Stitched model with	0.0	Stitched model with
Double	12.8	2 mm pitch	0.9	12 mm pitch
Ultimate failure strength				
Single	12.4	Stitched model with	4.1	Stitched model with
Double	17.5	2 mm pitch	6.4	12 mm pitch

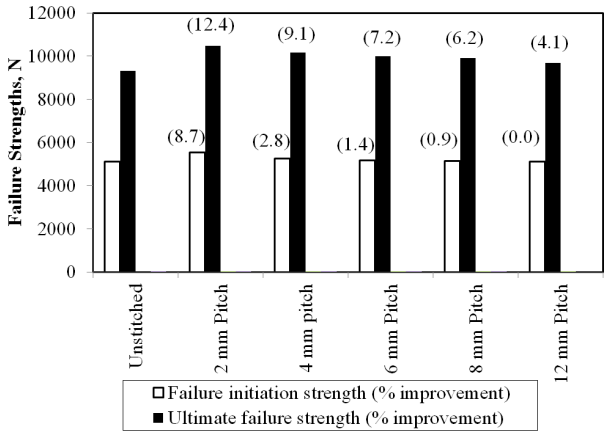

a) Single lap

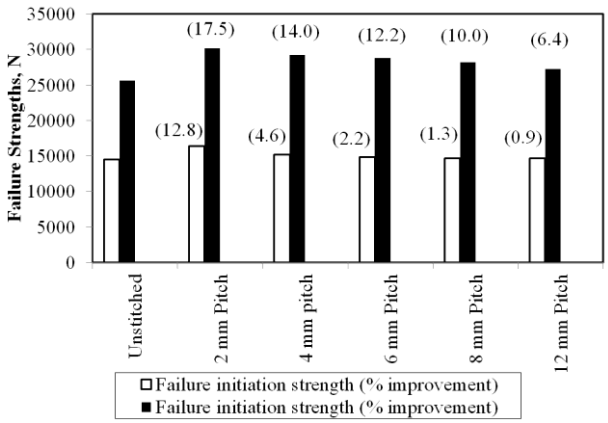

b) Double lap

Fig. 12: Failure strengths comparison

3.2. Effect of stitching material

To study the effect of stitch material, the single lap joint with 2 mm stitching pitch was tested with two other stitch materials namely carbon and glass fibers [19]. Results indicate that stitch material has negligible effect on the ultimate failure strengths as the lap joints will fail before the stitches reach their yield limit. However the failure initiation strength is directly sensitive to the Young's modulus of the stitch material.

3.3. Selective stitching

The single lap joint with 2 mm stitching pitch was further studied for selective stitching; where in non-uniform stitching is applied. The edges of the overlap are critical and hence are designed with finer stitch density and the center of the overlap is designed with coarser stitch density. Stitches were modified to arrive at the models as shown in Figs. 13 and 14. In all the selectively stitched models, the failure behaviour is observed to be similar to that of uniform stitched model. The improvement in failure strengths with respect to unstitched are shown in Fig. 15.

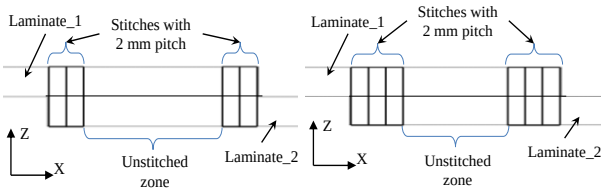

Model 1 **Model 2**

Fig. 13: Selective stitching models 1 & 2

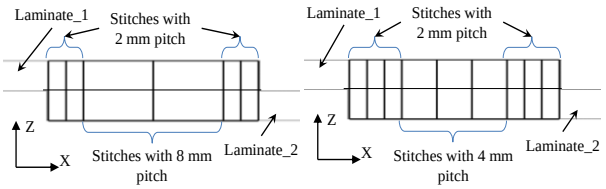

Model 3 **Model 4**

Fig. 14: Selective stitching models 3 & 4

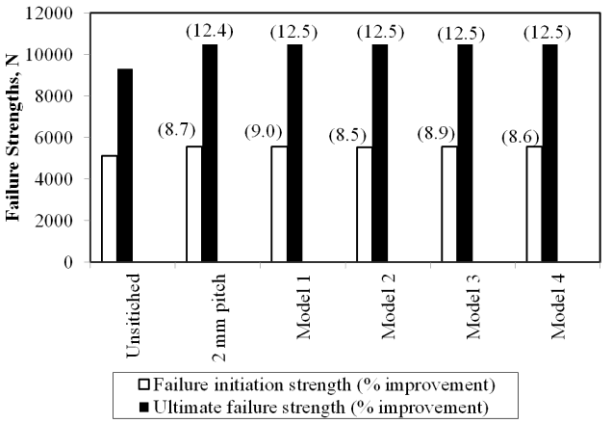

Fig. 15: Failure strengths of single lap models with selective stitching

4. Conclusion

The initial and ultimate failure strengths of single and double lap joints have been improved by through the thickness stitching. This is due to the significant reduction of inter-laminar S_{33} stresses in the presence of stitches which delays the initiation of the inter-laminar failure. The improvement in strengths is highly sensitive to the stitch density and is significant for pitch of less than 6mm. The failure initiation strengths are sensitive to the stitch fiber material; whereas ultimate failure strength is not affected. Hence if the failure initiation strength is not critical, suitable low cost stitch material like glass fiber can also be used to arrive at the same levels of ultimate failure strengths. The selective stitching analysis results show that presence of stitches at the edges of the lap is sufficient to increase the failure strength of the lap joints. The stitches at the center of the overlap have no significant effect on the model behaviour and hence can be avoided.

ACKNOWLEDGMENTS:

Authors would like to thank Prof. K.P. Rao, Mr. T.G.A. Simha, Mr. Madhusudhanan Nair, Mr. V.N. Divakaran and Dr. N. Sharma Rao for their technical guidance and review. Without their support this work could not have been completed. Authors also would like to thank Mr. P. Sundaresan for his valuable review.

REFERENCES:

[1] L. Tong, A.P. Mouritz and M.K. Bannister. 2002. *3D Fiber Reinforced Polymer Composites*, Elsevier Science.

[2] M. Karahan, Y. Ulcay, N. Karahan and A. Kuş. 2013. Influence of stitching parameters on tensile strength of Aramid/Vinyl Ester composites, *Materials Science*, 19(1). http://dx.doi.org/10.5755/j01.ms.19.1.3829.

[3] N. Zhao, H. Rödel, C. Herzberg, S.L. Gao and S. Krzywinski. 2009. Stitched glass/PP composite, Part I: Tensile and impact properties, *Composites Part A: Applied Science and Manufacturing*, 40(5), 635-643 http: //dx.doi.org/10.1016/j.compositesa.2009.02.019.

[4] F. Blas and I. Fernández. 2001. Mechanical characterisation of carbon/epoxy composite materials manufactured by resin film infusion method with stitching reinforcement, *Low Cost Composite Structures*.

[5] Composite Materials Handbook. 2002. Polymer Matrix Composites Materials Usage, *Design, and Analysis*, MIL-HDBK-17-3F.

[6] H.T. Hahn 2002. *Design, Manufacturing and Performance of Stitched Stiffened Composite Panels with and without Impact Damage*, U.S. Department of Transportation, Federal Aviation Administration.

[7] A. Aktas, P. Potluri and I. Porat. 2009. Multi-needle stitched composites for improved damage tolerance, *Proc. 17th Int. Conf. Composite Materials*, Edinburgh, Scotland.

[8] L.E. Stanley and D.O. Adams. 2001. *Development and Evaluation of Stitched Sandwich Panels*, NASA/CR-2001-211025.

[9] F. Pang and C.H. Wang. 2000. A predictive creep model for un-stitched and stitched woven composites, *Composites Science and Technology*, 60, 255-261. http:// dx.doi.org/10.1016/S0266-3538(99)00117-7.

[10] V. Carvelli, V. Koissin, J. Kustermans, S.V. Lomov, V.N. Tomaselli, B.V.D. Broucke, I. Verpoest and V. Witzel. 2009. Progressive damage in stitched composites: Static tensile tests and tension-tension fatigue, *Proc. 17th Int. Conf. Composite Materials*, Edinburgh, Scotland.

[11] Y. Tan, G. Wu, S.S. Suh, J.M. Yang, H.T. Hahn. 2008. Damage tolerance and durability of selectively stitched stiffened composite structures, *Int. J. Fatigue*, 30(3), 483-492.

[12] W. Trabelsi, L. Michel and R. Othomene. 2010. Effects of stitching on delamination of satin weave carbon-epoxy laminates under mode I, mode II and mixed-mode I/II loadings, *Applied Composite Materials*, 17(6), 575-595 http://dx.doi.org/10.1007/s10443-010-9128-0.

[13] E.H. Glaessgen and I.S. Raju.1999. Three-dimensional effects in the plate element analysis of stitched textile composites, *Proc. 40th AIAA/ASME/ASCE/AHS/ASC Structures, Structural Dynamics and Materials Conf. and Exhibit*, St. Louis, USA.. http://dx.doi.org/10.2514/6. 1999-1416.

[14] T. Rys, L. Chen and B. Sankar. 2010. Mixed mode fracture toughness of laminated stitched composites, *J. Reinforced Plastics and Composites*, 29(3), 422-430. http://dx.doi.org/10.1177/0731684408099407.

[15] M. Rathinasabapathy and S.B. Biggers. 2004. Finite element simulation of through-thickness stitching as a means for delamination growth control, *Proc. ABAQUS Users' Conf.*, Boston, Massachusetts.

[16] B.K. Fink, A.M. Monib, and J.W. Gillespie Jr. 2001. *Damage Tolerance of Thick-Section Composites Subjected to Ballistic Impact*, ARL-TR-2477.

[17] ABAQUS V6.11 Documentation.

[18] S.W. Tsai. 1992. *Theory of Composites Design*, Stanford University.

[19] J.E. Mark. 2007. *Physical Properties of Polymers Handbook*, Springer.